

Large influence of capping layers on tunnel magnetoresistance in CoFe/MgO/CoFe magnetic tunnel junctions

Jiaqi Zhou,^{a,b} Weisheng Zhao,^{*a,b} Yin Wang,^c Shouzhong Peng,^{a,b} Junfeng Qiao,^{a,b} Li Su,^{a,b,d} Lang Zeng,^{a,b} Na Lei,^{a,b} Youguang Zhang^{a,b} and Arnaud Bournel^d

^a Fert Beijing Institute, Beihang University, Beijing 100191, China.

^b School of Electronic and Information Engineering, Beihang University, Beijing 100191, China.

^c Department of Physics and the Center of Theoretical and Computational Physics, The University of Hong Kong, Pokfulam Road, Hong Kong SAR, China.

^d Institut d'Electronique Fondamentale, Université Paris-Sud, Université Paris-Saclay, CNRS, F-91405 Orsay, France.

*Email: weisheng.zhao@buaa.edu.cn

Abstract

We report the first-principles theoretical investigations of the tunnel magnetoresistance(TMR) effect in the symmetric capping layer/CoFe(001)/MgO(001)/CoFe(001)/capping layer magnetic tunnel junctions(MTJs) with Ta, Hf and Ir used as capping layer materials. Spin-resolved conductance and TMR ratios are shown and it is found that the TMR ratio is sensitive to the capping layer material. The spin polarization of *s* state in Co atom at the CoFe/capping layer interface is presented to explain the influence on TMR ratio caused by different capping layers, and we can obtain a high spin polarization value and a giant TMR ratio when Ir is used, demonstrating that Ir is an ideal capping layer material. We also study the spin-polarized transport properties in the Brillouin zone. In the parallel condition, a central broad peak is found in the majority-spin channel due to the Δ_1 state, while sharp transmission probability peaks at some \mathbf{k}_{\parallel} -points appear in the minority-spin channel. The sharp peak phenomenon is attributed to the resonant tunnel transmission effect and the projected density of states (PDOS) is shown for analysis.

1. Introduction

Spin-transfer-torque magnetic random access memories(STT-MRAMs) are characterized by several merits such as non-volatility, high density and low power consumption.¹ The information is stored by the orientation of the magnetization in nanometre-scale ferromagnetic elements, called magnetic tunnel junctions (MTJs).² The tunnel magnetoresistance(TMR) phenomenon observed in the MTJ has been investigated theoretically and experimentally for decades.²⁻⁴ Thanks to rapid advances in the growth technique of ultra-thin ferromagnetic films, MTJs with high TMR ratios based on CoFeB/MgO have been achieved⁵⁻¹⁰ after the prediction of the first-principles calculations.¹¹

Since the first-principles theory successfully explained the high TMR in the MTJ,¹¹ a great deal of progress has been achieved in this field. Butler *et al.* provided a thorough explanation of the physics behind the TMR of Fe/MgO/Fe by a Korringa–Kohn–Rostoker (KKR) technique, connecting it with the symmetry match of the Bloch states between the electrode and the MgO barrier.¹² After that, Zhang *et al.* reported the TMR investigation in body-centered cubic (bcc) Co/MgO/Co and FeCo/MgO/FeCo tunnel junctions, noting that the total reflection depends on the absence of the Δ_1 band for the minority spin in the cubic (100) direction, and predicted a high TMR ratio in the MTJ based on FeCo.¹³ Later, Waldron *et al.* studied the voltage dependence of TMR in the Fe/MgO/Fe MTJ at non-equilibrium

state, indicating that the quench of TMR by bias was due to a relatively fast increase of channel currents in the anti-parallel condition.¹⁴ Besides, abundant studies have demonstrated that subtle details at the interface would influence TMR and spin properties of the MTJ, such as vacancy defects at the interface boundary, the oxidation at the interface, the presence of interface resonant states, etc.¹⁵⁻¹⁷

In addition to TMR, another important device trait of the MTJ is the perpendicular magnetic anisotropy (PMA) which is significant to achieve high thermal stability in the nano-scale device. The PMA observed in MgO/CoFeB/metallic capping layer structures has been investigated extensively¹⁸⁻²² and it has been demonstrated that the PMA of CoFeB/MgO-based structures is critically dependent on the capping layer materials.²³⁻²⁶ Although the influence on TMR caused by capping layers has been studied in the aspect of diffusion,²⁷⁻²⁸ the investigation on the interfacial effect at the CoFe/capping layer interface is insufficient, and in CoFe/MgO/CoFe MTJ, the essential influence on TMR caused by capping layers remains unclear, which leads to the difficulty in TMR optimization for MTJ nano-pillars. In this paper, we focus on the influence on TMR and spin polarization caused by capping layer and analyse the interfacial states at CoFe/capping layer interfaces. It is found that capping layers have large influence on the *s* state spin polarization of Co atom at the interface, and further impact the TMR ratio.

2. Calculation details

We report a first-principles study of the spin dependent transport in X/CoFe(001)/MgO(001)/CoFe(001)/X MTJ nano-pillar, where X represents the capping layer material Ir, Ta or Hf as strong PMA can be achieved in MgO/CoFeB/X structures.^{19,22,25} The atomic structure is illustrated in Fig. 1. It is a two-probe MTJ, composed of two semi-infinite capping layer materials X electrodes sandwiching X/CoFe/MgO/CoFe/X ultra-thin structure. The x-y lattice constant of the junction is fixed to 2.83 Å. Atomic structures of central region have been relaxed by Vienna ab initio simulation package(VASP),²⁹ and the optimized distance from the interfacial X layer to the closest Co layer is respectively 1.711 Å, 1.748 Å or 1.844 Å when X represents Ir, Ta or Hf.

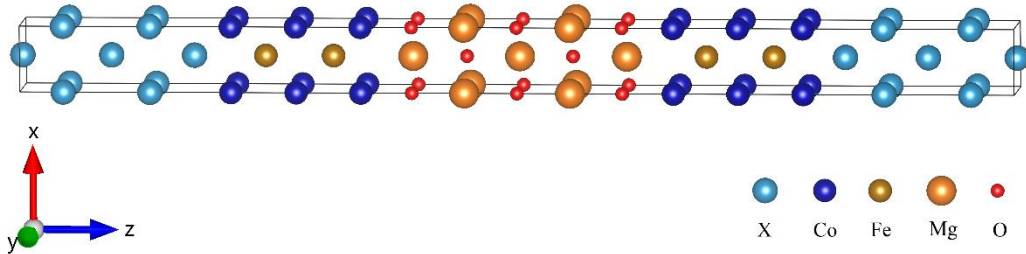


Fig. 1 Atomic structure of an X/CoFe/MgO/CoFe/X MTJ model, X represents the capping layer material Ir, Ta or Hf. The transport direction is along the z-axis while the MTJ is periodic along the x- and y-directions.

Quantum transport properties are calculated by a state-of-the-art technique based on density functional theory (DFT) combined with Keldysh non-

Equilibrium Green's function(NEGF) formalism^{30,31} as implemented in the NanoDCAL package which is based on linear combination of atomic orbital (LCAO) basis sets made of double-zeta plus polarization orbital (DZP) basis functions. The spin-resolved conductance is given by Landauer-Büttiker formula

$$G_\sigma = \frac{e^2}{h} \sum_{\mathbf{k}_\parallel} T_\sigma(\mathbf{k}_\parallel, E_F) \quad (1)$$

where $T_\sigma(\mathbf{k}_\parallel, E_F)$ is the transmission coefficient with spin σ at the transverse Bloch wave vector $\mathbf{k}_\parallel = (k_x, k_y)$ and the Fermi level E_F , e is the electron charge, and h is the Planck constant. The spin-resolved transmission coefficient at E_F is calculated by

$$T_\sigma(E_F) = \text{Tr}[\Gamma_L(E_F)G^r(E_F)\Gamma_R(E_F)G^a(E_F)]_{\sigma\sigma} \quad (2)$$

where G^r and G^a are respectively retarded and advanced Green's functions of the system; Γ_α ($\alpha = L, R$) is the linewidth function which describes the coupling between the α lead and the scattering region.³² We found a 20×20 k-point mesh sufficient for self-consistent calculations of this two-probe device and a much denser sampling 500×500 was further used for calculation of transmission coefficient of all spin channels.³³ The mesh cut-off energy was 3000 eV, high enough for our calculations, and energy tolerance for self-consistency was restricted to 10^{-5} eV.

TMR ratio is defined as

$$TMR = \frac{G_{PC} - G_{APC}}{G_{APC}} \quad (3)$$

where G_{PC} and G_{APC} are the total conductance for the magnetizations of two ferromagnetic layers in the parallel configuration(PC) and the anti-parallel configuration(APC), respectively.

The spin polarization of atoms at E_F is defined as

$$SP = \frac{N_{\uparrow}(E_F) - N_{\downarrow}(E_F)}{N_{\uparrow}(E_F) + N_{\downarrow}(E_F)} \quad (4)$$

where $N_{\uparrow}(E_F)$ and $N_{\downarrow}(E_F)$ are respectively the majority- and minority-spin density of states(DOS) at E_F .

3. Results and discussion

Firstly, we investigated the spin-resolved transport properties in PC and APC of MTJ nano-pillars with three different capping materials. The conductance and TMR ratios are shown in Table 1. It is found that TMR ratios of all three MTJ nano-pillars are pretty high and this phenomenon is attributed to the Δ_1 spin-filtering effect. Namely, for bcc CoFe(001), only the Δ_1 band in the majority spin crosses E_F , while for MgO tunnel barrier, Δ_1 evanescent states have the slowest decay. When the symmetries of tunnel wave functions are conserved, Δ_1 Bloch states in CoFe couple with Δ_1 evanescent states in MgO tunnel barrier, dominating the majority channel tunnel conductance in PC.^{13,34,35} We have found that there are Δ_1 channels in all three capping materials, meaning that Δ_1 Bloch states would pass through X capping layers, therefore a large conductance difference between PC and APC is obtained and leads to a high TMR ratio. It is also shown that the TMR ratio of Ir-cap MTJ is much higher than that of both

Ta-cap and Hf-cap MTJs due to the high majority-spin conductance in PC and the low conductance in APC. In addition, by comparing the values of $G_{PC}^{\uparrow\uparrow}$ and $G_{PC}^{\downarrow\downarrow}$ which are the majority-spin and minority-spin conductance in PC respectively, we acquire some interesting results. $G_{PC}^{\uparrow\uparrow}$ are about one order of magnitude larger than $G_{PC}^{\downarrow\downarrow}$ in both Ir-cap MTJ and Hf-cap MTJ. However, the case is different in Ta-cap MTJ where the $G_{PC}^{\downarrow\downarrow}$ is larger than $G_{PC}^{\uparrow\uparrow}$, which would be explained in the following.

TABLE 1. The calculated spin-polarized conductance G_σ (in units of e^2/h) and TMR ratios (in %) for three different MTJs. $G_{PC}^{\uparrow\uparrow}$, $G_{PC}^{\downarrow\downarrow}$ are the majority-spin and minority-spin conductance in PC respectively. $G_{APC}^{\uparrow\downarrow}$, $G_{APC}^{\downarrow\uparrow}$ are the majority-to-minority and minority-to-majority conductance in APC respectively.

structure	$G_{PC}^{\uparrow\uparrow}$	$G_{PC}^{\downarrow\downarrow}$	$G_{APC}^{\uparrow\downarrow}$	$G_{APC}^{\downarrow\uparrow}$	TMR
Ir/CoFe/MgO/CoFe/Ir	1.361×10^{-4}	2.898×10^{-5}	5.874×10^{-7}	5.836×10^{-7}	13997
Ta/CoFe/MgO/CoFe/Ta	6.859×10^{-5}	9.067×10^{-5}	1.813×10^{-6}	2.299×10^{-6}	3773
Hf/CoFe/MgO/CoFe/Hf	1.094×10^{-4}	1.460×10^{-5}	2.194×10^{-6}	1.908×10^{-6}	2923

To understand the conductance and TMR ratios, we investigated the transmission coefficient in the two-dimensional Brillouin zone(BZ) at E_F , as plotted in Fig. 2. The log function has been applied to the transmission coefficient, and the red(blue) color represents the high(low) transmission probability. For all the three X-cap MTJs, the majority spin in PC has a broad peak centered at $\mathbf{k}_\parallel = (0,0)$ due to the slow decay of the Δ_1 state,

whereas for the minority spin in PC and APC there are negligible transmission probabilities, except for some sharp peaks at special \mathbf{k}_{\parallel} points (see bright spots in red circles). For example, Fig. 2(e) shows that at $\mathbf{k}_{\parallel} = (0.56, 0.96)\pi/a$ the channel has a transmission coefficient larger than 0.4, indicating that electrons transmit through the MgO tunnel barrier with over 40% probability. This channel contributes to $G_{PC}^{\downarrow\downarrow}$ largely and lead that $G_{PC}^{\downarrow\downarrow}$ is large than $G_{PC}^{\uparrow\uparrow}$ in Ta-cap MTJ. Such a high transmission probability originates from the resonant tunnel.³⁶ This phenomenon occurs when localized interface states on the two CoFe/MgO interfaces align in energy. It can be confirmed by the partial density of states (PDOS) of a Co atom at the CoFe/X interface shown in Fig. 3 where the minority-spin DOS shows a clear peak at E_F , demonstrating the existence of interfacial states. This resonant tunnel transmission feature also appears when X is Ir or Hf, as shown in Fig. 2(b) at $\mathbf{k}_{\parallel} = (0.74, 0.81)\pi/a$ with the transmission coefficient of 0.08 and Fig. 2(h) at $\mathbf{k}_{\parallel} = (0.12, 0.97)\pi/a$ with 0.1, as shown in red circles.

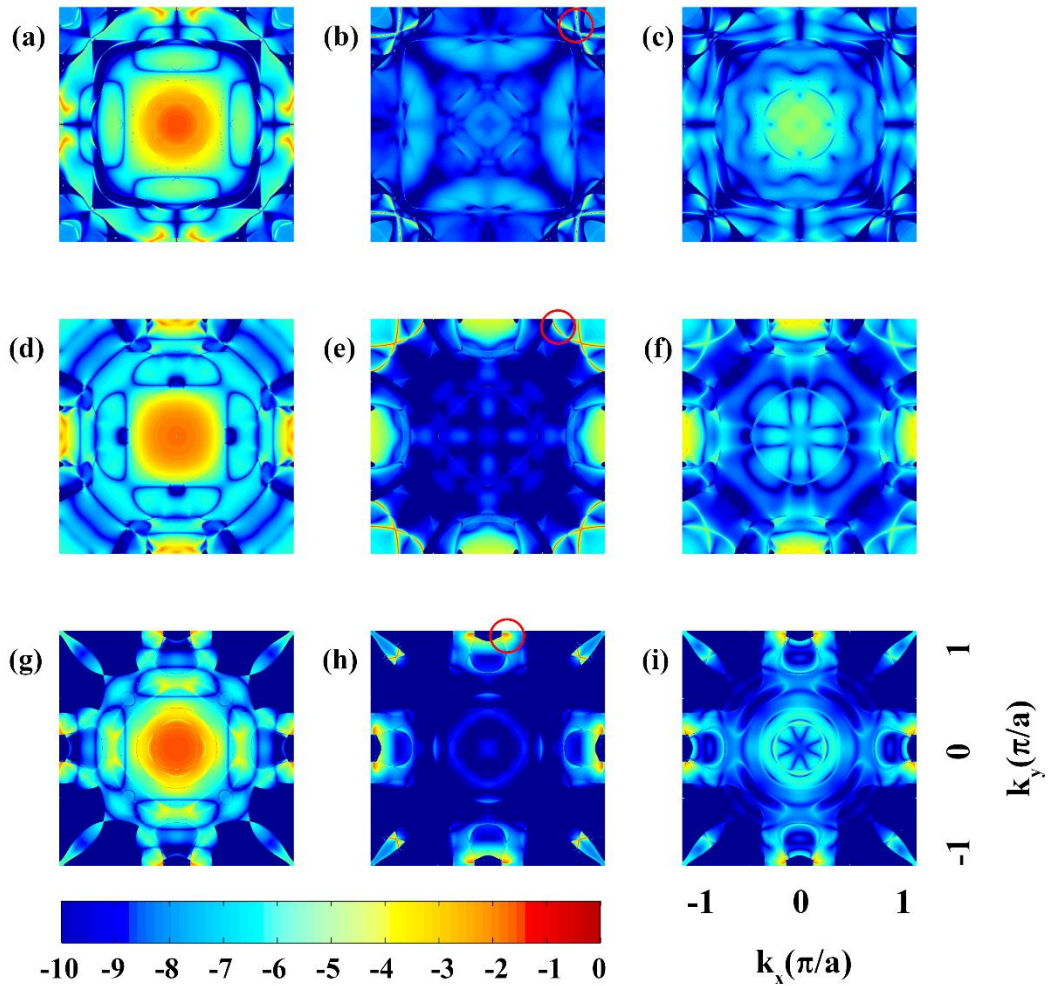


Fig. 2 Spin- and \mathbf{k}_{\parallel} -resolved transmission coefficients for ((a)-(c)) Ir/CoFe/MgO/CoFe/Ir, ((d)-(f)) Ta/CoFe/MgO/CoFe/Ta and ((g)-(i)) Hf/CoFe/MgO/CoFe/Hf at E_F . Panels from left to right are ((a), (d), (g)) for majority-to-majority in PC and ((b), (e), (h)) for minority-to-minority in PC; ((c), (f), (i)) for majority-to-minority or minority-to-majority in APC. Resonant tunnel transmission features are shown in red circles.

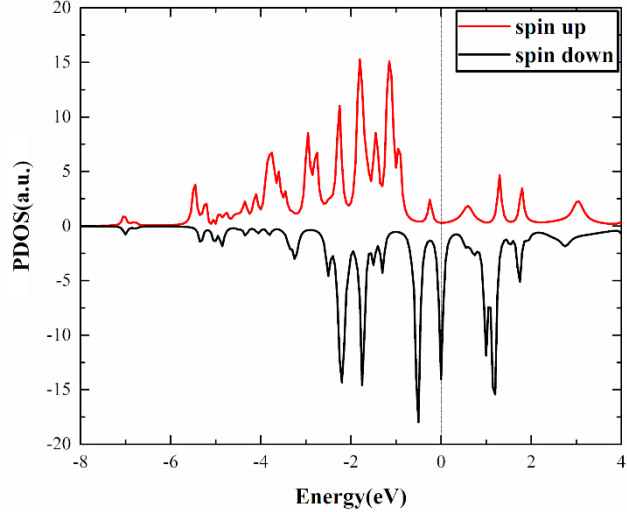


Fig. 3 Majority-spin (positive) and minority-spin (negative) partial density of states (in arbitrary units) at $\mathbf{k}_{\parallel}=(0.56, 0.96)\pi/a$ of Co atom at the CoFe/Ta interface. E_F is set to be zero.

In order to investigate the interfacial effects caused by different capping layer materials, we study the PDOS on different orbitals of Co atoms at the CoFe/X interface. It is known that only the Δ_1 wave functions are compatible with $l=0$ symmetry.¹³ The spin-resolved DOS of Co atom at the CoFe/X interface is illustrated in Fig. 4. The s state spin polarization for Co at the CoFe/Ir, CoFe/Ta and CoFe/Hf interface are 67%, 45% and 42% respectively, which agrees well with the trend of TMR ratios in the three structures. It has been reported that in bcc CoFe the Δ_1 Bloch states are highly spin-polarized³⁶ and the TMR ratio could reach up to $\sim 34000\%$.¹³ Due to the existence of the capping layer, the spin polarization of interfacial Co atom is damaged and the TMR ratio decline consequently.

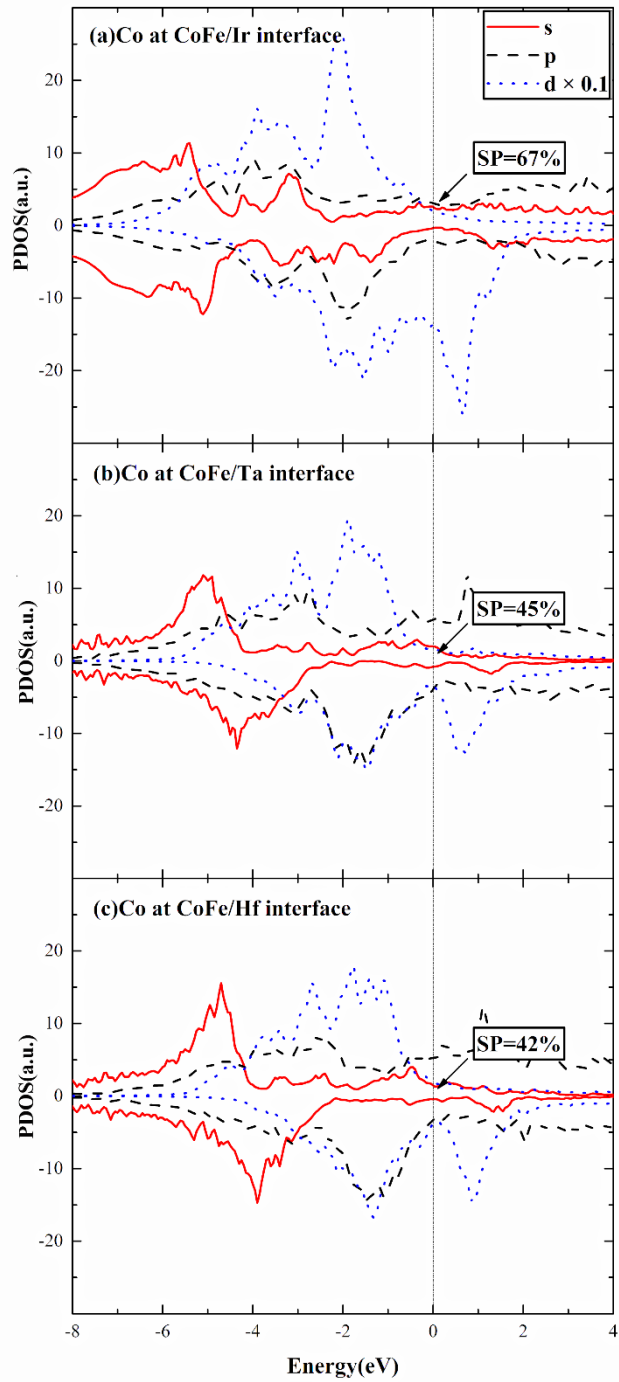


Fig. 4 Majority-spin (positive) and minority-spin (negative) partial density of states (in arbitrary units) on different orbitals of Co atom at the interface of (a) CoFe/Ir, (b) CoFe/Ta and (c) CoFe/Hf. E_F is set to be zero.

4. Conclusions

In summary, we investigated the spin-resolved conductance and TMR ratios in $X/\text{CoFe}(001)/\text{MgO}(001)/\text{CoFe}(001)/X$ MTJ with X electrodes, where X represents Ir, Ta or Hf capping layer material that can produce strong PMA effect in the $\text{MgO}/\text{CoFeB}/X$ structure. It is found that TMR ratios are sensitive to different capping layers and Ir is an ideal capping layer material to obtain a giant TMR. To explain the influence on TMR caused by different capping layers, we focused on the s state spin polarization of Co atom at the CoFe/capping layer interface. The spin polarization varies as the capping layer materials change, and the trend corresponds well to the TMR ratio in MTJs with different capping layers. As a result, we believe that the capping layers influence the s state spin polarization and then impact the TMR largely. The spin-resolved transport properties were also calculated in BZ. We found that in the majority-spin transport channel the Δ_1 state plays the dominant role, while in the minority-spin transport channel the resonant transmission happens at some \mathbf{k}_{\parallel} -points, contributing to the $G_{PC}^{\downarrow\downarrow}$ greatly. The PDOS figure shows an obvious sharp peak at E_F in the minority spin, demonstrating this phenomenon further.

Acknowledgements

The authors gratefully acknowledge the International Collaboration Project 2015DFE12880 from the Ministry of Science and Technology in China, National Natural Science Foundation of China (Grant No. 61571023, 61501013 and 61471015), and Beijing Municipal of Science and Technology (Grant No. D15110300320000) for their financial support of this work. We thank Dr. Yibin Hu for fruitful discussions.

Reference

- 1 A. D. Kent and D. C. Worledge, *Nat. Nanotechnol.*, 2015, **10**, 187–191.
- 2 C. Chappert, A. Fert and F. N. Van Dau, *Nat. Mater.*, 2007, **6**, 813–823.
- 3 H. Gu, X. Zhang, H. Wei, Y. Huang, S. Wei and Z. Guo, *Chem. Soc. Rev.*, 2013, **42**, 5907–5943.
- 4 J. S. Moodera, L. R. Kinder, T. M. Wong and R. Meservey, *Phys. Rev. Lett.*, 1995, **74**, 3273–3276.
- 5 S. Yuasa, T. Nagahama, A. Fukushima, Y. Suzuki and K. Ando, *Nat. Mater.*, 2004, **3**, 868–871.
- 6 S. S. P. Parkin, C. Kaiser, A. Panchula, P. M. Rice, B. Hughes, M. Samant and S.-H. Yang, *Nat. Mater.*, 2004, **3**, 862–867.
- 7 D. D. Djayaprawira, K. Tsunekawa, M. Nagai, H. Maehara, S. Yamagata, N. Watanabe, S. Yuasa, Y. Suzuki and K. Ando, *Appl. Phys. Lett.*, 2005, **86**, 092502.
- 8 S. Ikeda, J. Hayakawa, Y. Ashizawa, Y. M. Lee, K. Miura, H. Hasegawa, M. Tsunoda, F. Matsukura and H. Ohno, *Appl. Phys. Lett.*, 2008, **93**, 082508.
- 9 J. Hayakawa, S. Ikeda, Y. M. Lee, F. Matsukura and H. Ohno, *Appl. Phys. Lett.*, 2006, **89**, 232510.

10 Y. M. Lee, J. Hayakawa, S. Ikeda, F. Matsukura and H. Ohno, *Appl. Phys. Lett.*, 2007, **90**, 212507.

11 J. Mathon and A. Umerski, *Phys. Rev. B: Condens. Matter*, 2001, **63**, 220403.

12 W. H. Butler, X.-G. Zhang, T. C. Schulthess and J. M. MacLaren, *Phys. Rev. B: Condens. Matter*, 2001, **63**, 054416.

13 X.-G. Zhang and W. H. Butler, *Phys. Rev. B: Condens. Matter*, 2004, **70**, 172407.

14 D. Waldron, V. Timoshevskii, Y. Hu, K. Xia and H. Guo, *Phys. Rev. Lett.*, 2006, **97**, 226802.

15 Y. Ke, K. Xia and H. Guo, *Phys. Rev. Lett.*, 2010, **105**, 236801.

16 V. Timoshevskii, Y. Hu, É. Marcotte and H. Guo, *J. Phys. Condens. Matter*, 2014, **26**, 015002.

17 B. S. Tao, H. X. Yang, Y. L. Zuo, X. Devaux, G. Lengaigne, M. Hehn, D. Lacour, S. Andrieu, M. Chshiev, T. Hauet, F. Montaigne, S. Mangin, X. F. Han and Y. Lu, *Phys. Rev. Lett.*, 2015, **115**, 157204.

18 W.-G. Wang, M. Li, S. Hageman and C. L. Chien, *Nat. Mater.*, 2011, **11**, 64–68.

19 S. Ikeda, K. Miura, H. Yamamoto, K. Mizunuma, H. D. Gan, M. Endo, S. Kanai, J. Hayakawa, F. Matsukura and H. Ohno, *Nat. Mater.*, 2010, **9**, 721–724.

20 Z. Wang, M. Saito, K. P. McKenna, S. Fukami, H. Sato, S. Ikeda, H. Ohno and Y. Ikuhara, *Nano Lett.*, 2016, **16**, 1530–1536.

21 P. G. Gowtham, G. M. Stiehl, D. C. Ralph and R. A. Buhrman, *Phys. Rev. B: Condens. Matter*, 2016, **93**, 024404.

22 W. Skowronski, T. Nozaki, Y. Shiota, S. Tamaru, K. Yakushiji, H. Kubota, A. Fukushima, S. Yuasa and Y. Suzuki, *Appl. Phys. Express*, 2015, **8**, 053003.

23 S. Peng, M. Wang, H. Yang, L. Zeng, J. Nan, J. Zhou, Y. Zhang, A. Hallal, M. Chshiev, K. L. Wang, Q. Zhang and W. Zhao, *Sci. Rep.*, 2015, **5**, 18173.

24 Y.-W. Oh, K.-D. Lee, J.-R. Jeong and B.-G. Park, *J. Appl. Phys.*, 2014, **115**, 17C724.

25 T. Liu, J. W. Cai and L. Sun, *AIP Adv.*, 2012, **2**, 032151.

26 M.-S. Jeon, K.-S. Chae, D.-Y. Lee, Y. Takemura, S.-E. Lee, T.-H. Shim and J.-G. Park, *Nanoscale*, 2015, **7**, 8142–8148.

27 H. Almasi, D. R. Hickey, T. Newhouse-Illige, M. Xu, M. R. Rosales, S. Nahar, J. T. Held, K. a. Mkhoyan and W. G. Wang, *Appl. Phys. Lett.*, 2015, **106**, 182406.

28 T. Miyajima, T. Ibusuki, S. Umehara, M. Sato, S. Eguchi, M. Tsukada and Y. Kataoka, *Appl. Phys. Lett.*, 2009, **94**, 122501.

29 G. Kresse and J. Furthmuller, *Phys. Rev. B: Condens. Matter*, 1996, **54**, 11169.

30 J. Taylor, H. Guo and J. Wang, *Phys. Rev. B: Condens. Matter*, 2001, **63**, 245407.

31 J. Taylor, H. Guo and J. Wang, *Phys. Rev. B: Condens. Matter*, 2001, **63**, 121104.

32 B. Wang, J. Li, Y. Yu, Y. Wei, J. Wang and H. Guo, *Nanoscale*, 2016, **8**, 3432–3438.

33 L. L. Tao, S. H. Liang, D. P. Liu, H. X. Wei, J. Wang and X. F. Han, *Appl. Phys. Lett.*, 2014, **104**, 172406.

34 S. Yuasa and D. D. Djayaprawira, *J. Phys. D. Appl. Phys.*, 2007, **40**, R337–R354.

35 W. H. Butler, X.-G. Zhang, S. Vutukuri, M. Chshievand and T. G. Schulthess, *IEEE Trans. Magn.*, 2005, **41**, 2645–2648.

36 S. Yuasa, T. Nagahama and Y. Suzuki, *Science*, 2002, **297**, 234–237.